ACTA STEREOL 1998; 17/2: 237-246
ORIGINAL SCIENTIFIC PAPER

3D VORONOI TESSELLATIONS OF CLUSTER FIELDS

Ivan Saxl, Petr Ponížil *

Mathematical Institute, Acad. Sci. of the Czech Republic, Žitná 25, CS-115 67 Praha 1, Czech Republic
*TU Brno, Faculty of Technology, náměstíTGM 275, CS-762 72 Zlín, Czech Republic

ABSTRACT

Spatial Voronoi tessellations generated by cluster fields of the Neyman-Scott type and the sectional 2D induced tessellations were simulated. The effect of number and arrangement of points forming the cluster and of the cluster size on several tessellation characteristics is explained using the concept of inner and outer cells filling the cluster core and the space between clusters, respectively.

Key Words: cell characteristics, cluster fields, 3D Voronoi tessellation

INTRODUCTION

Random tessellations are an important tool of the examinations of objects scattered in the space. The investigated object is often a natural planar or spatial tessellation, as in the case of districts of administrations, thin monolayers of bubbles or biological cells and, in particular, in the case of polycrystalline grains. Also planar or spatial point patterns are examined and in order to describe or to optimize their arrangement, tessellations induced by them are analyzed and compared with theoretical models.
Clustering of particles or space-filling cells is a wide-spread phenomenon connected with local inhomogeneities of the embedding natural space. The present paper is devoted to the cluster fields of the Neyman-Scott type which are constructed as follows. First a pattern of points called *the parents* is chosen; the usual choice is the stationary Poisson point process (PPP) of intensity λ_p. Further, a random cluster $Z = \{z_1, \ldots, z_m\}$ of points called *the daughters* is defined by prescribing the distribution law of their number m and of their spatial arrangement. Mutually independent clusters are then implanted in the parent points and the union of daughters constitutes the cluster field; its intensity is $\lambda = N\lambda_p$. Such cluster fields can also be called Boolean as their construction is similar to the generation of Boolean model with the grains being random point clusters. Two cases of the daughter arrangement will be considered here; the daughters are scattered uniformly at random either within a ball of diameter D - *globular (G) clusters*, or, at the sphere of diameter D - *spherical (S) clusters*. Beside the ordinary choice, namely m is Poisson distributed with the mean value N - *Poisson (P) clusters*, also the case of the fixed daughter number $m \equiv N$

Research supported by the Grant Agency of the Czech Republic (grant 201/96/0226).

- *binomial (B) clusters* - will be considered in the case of globular clusters. Poisson clusters are a mixture of clusters with various $m = 0, 1, ...$ and the fraction of void clusters is $\exp(-N)$. At $N = 1$, the binomial cluster field is the parent PPP, whereas the Poisson cluster field approaches even at $D \to 0$ an independently thinned PPP of intensity $\lambda_p(1 - \exp(-N))$. Several properties (K-function, pair correlation function, nearest neighbour and spherical distance distribution functions) of these cluster fields can be calculated theoretically (Stoyan *et al.*, 1995; Rataj and Saxl, 1997). Unfortunately, data concerning 3D cluster field tessellations are rather scarce; they are missing in the monograph by Okabe *et al.* (1992), examples of Poisson globular cluster field (PGCF, called also Matérn cluster field) are in Lorz (1990), Lorz and Hahn (1993) and Hahn and Lorz (1994). Only few selected cases have been analysed there in order to compare them with the Poisson-Voronoi tessellation (PVT).

PRELIMINARY CONSIDERATIONS

The tessellation properties can be divided according to their behaviour with respect to the changes in the intensity of the underlying point process λ. The *size characteristics* are homogeneous functions of degree $k, k > 0$, of λ - $f(\alpha\lambda) = \alpha^k f(\lambda)$; $k = -1, -\frac{2}{3}$ and $-\frac{1}{3}$ for the cell volume v, cell surface area s and for cell perimeter p as well as the mean cell breadth w, respectively. Consequently, the unit density of the daughter process λ is assumed in all numerical results that follow and a dimensionless cluster size parameter is introduced, namely the ratio $c = D/(\mathbf{E}\rho_p)$, where $\mathbf{E}\rho_p = 0.55\lambda_p^{-1/3}$ is the mean nearest neighbour distance of parents. On the other hand, $k = 0$ for the *shape characteristics* like mean dihedral angle Θ, randomly selected dihedral angle θ, number of cell faces n and cell shape factors $g = 6v\sqrt{\pi/s^3}, f = 6v/(\pi w^3)$, ($g = f = 1$ for a ball).

When the cluster size is very small and the mean number N is also small, the cell of the tessellation induced by parents either vanishes ($m = 0$) or is divided into $m > 0$ subcells of a comparable size with a nearly unchanged outer common boundary of the parent cell. The shrinkage of clusters below some size does not influence this division substantially. Consequently, the average tessellation characteristics change only slowly with D decreasing further below a certain value. At the same time, several new faces are created and, consequently, the cell surface area as well as cell perimeter increase. Simultaneously, the original parent cells with the average value of $\mathbf{E}w = 1.458$ are flattened to a certain degree and therefore the average mean breadth $\mathbf{E}w$ also increases. The distributions of size properties are changed and the variances of properties increase in comparison with the parent PVT but the modes shift only slightly because of the normalization to $\lambda = 1$.

When the cluster size is still small and the mean number N is higher, small *inner cells* can develop with the neighbours being generated by daughters of the same cluster; their fraction q will be an increasing function of N. Their mean volume will be roughly proportional to the reciprocal value of the local intensity in the cluster $\lambda_d = 6N/(\pi D^3) = 11.23\lambda c^{-3} \equiv \alpha\lambda$. The higher is N the better will the distribution of size characteristics of these inner cluster cells imitate the distribution of the properties of the parent PVT cells. The daughters lying near the boundary of the cluster embedding ball will generate *outer cells* similar to those created by clusters with a small mean daughter number N. Consequently, the resulting distributions of the cell size property M will be bimodal. The primary mode will roughly correspond to the PVT of the intensity $(1 - q)\lambda$ and with increasing N shifts from the position of $x_{PVT}(\lambda; M)$ to

higher values; the height of the primary maximum decreases. The secondary mode will be $\alpha^{k/3}x_{PVT}(\lambda; M)$, where k is the degree of the homogeneity of the property M, hence shifted very far to the left from $x_{PVT}(\lambda; M)$ if c is small. The height of the p.d.f. in the mode will be proportional to q and to $\alpha^{-k/3}$.

In any case, the original increase in the mean values of the size properties will be stopped and their decrease can be expected with growing fraction q of small inner cells. Consequently, a maximum of the mean values of these properties occurs at some value of N. On the other hand, with growing N, a monotone increase of variances is ensured as the increasing number of small inner cells is compensated by gradually greater outer cells.

Let N be kept fixed at some selected value and let the cluster size c start to increase from some negligible value, 0.005 say. First the clusters grow without mutual interaction; the local intensity λ_d decreases proportionally to c^{-3}, the secondary modes shift to higher values and their heights continually decreases. Then, in the intermediate range of cluster sizes, overlap of clusters takes place. Its degree can be estimated as follows. The probability that a ball C of diameter $D = 0.55c/\lambda_p^{1/3}$ centred in a point of the parent Poisson point process has a non-void intersection with another such ball is $p_1 = 1 - \exp[-4\pi\lambda_p D^3/3] = 1 - \exp[-(0.893c)^3]$ (Stoyan *et al.*, 1995). Similarly $p_2 = 1 - \exp[-\pi\lambda_p D^3/6] = 1 - \exp[-(0.4465c)^3]$ is the probability that C contains the centre of another such ball. Consequently, p_1 and p_2 are rough measures of mild and deep cluster overlapping, respectively. To $c \leq 0.5$ correspond the values $p_1 \leq 0.1$, $p_2 \leq 0.01$, hence the overlapping (interaction) of clusters is negligible - *cluster size range I* (the range of the growth without interaction). On the other hand, if $c \geq 4$ then $p_1, p_2 \sim 1$ and the clusters are dispersed - *size range III* - the cluster field in certain sense approach the Poisson point process of intensity λ. In the *intermediate range II,* $0.5 \leq c \leq 4$, the major changes of tessellation characteristics are therefore expected. Very large as well as very small cells vanish here, the variances of the size properties decrease accordingly. The mean values will approach the values appropriate for PVT; hence they will decrease for small values of N and increase for high values of N.

All these predictions based on the existence of inner and outer cells relate only to tessellations produced by globular clusters. In tessellations produced by spherical clusters, the presence of inner cells would be rather exceptional unless N is very high. The secondary minima will be suppressed to a great extent and perhaps also misplaced in comparison with the previous case. Then also a monotone increase of the mean values as well as of the variances of the size characteristics is anticipated.

RESULTS OF SIMULATIONS

Beside PGCF's also binomial globular (BGCF) and Poisson spherical (PSCF) cluster fields of the unit intensity $\lambda = 1/\mathbf{E}v = 1$ have been generated. Simultaneously with 3D tessellations, also their 2D planar sections were examined. The range of variables was $1 \leq N \leq 30$ (at $N = 1$, 37% of Poisson clusters is void and 37% contains 1 daughter only) and $0.005 \leq c \leq 10$. Edge effects have been carefully removed and each realization contained approximately 1000 cells for statistical examination. The total number of realizations was about 3000 for each choice of independent variables c, N. Consequently, 3.10^6 cells and their 2D profiles have been analysed in each case. The spherical clusters produce degenerate Voronoi cells (*i.e.* more than 4 edges meet in a vertex) in the centre of the embedding ball. In order to avoid this, any daughter was

given an independent small shift with random components s_x, s_y, s_z; the components were independent normal with the mean 0 and variance $\sigma^2 = (0.00002)^2$ (in the same units as the size parameter c). It cannot be excluded that random oscillations of daughters produce a slightly higher proportion of inner cells at $c = 0.005$ and $N \geq 20$.

a) The effect of variable mean number of daughters N.

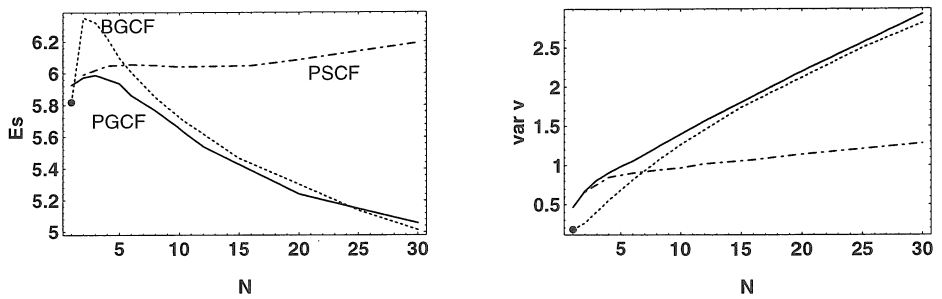

a) b)

Fig. 1 The mean cell surface s (a) and the variance of the cell volume v(b). The behaviour of the mean width w and of the perimeter p is very similar. The circle at $N = 1$ denotes the PVT value.

The mean values of cell size characteristics in the tessellations generated by globular clusters behave very similarly; a maximum occurring at $N = 2$ or $N = 3$ (sharp in BGCF and shallow in PGCF tessellations) is followed by a steady decrease - Fig. 1a. The height of the maximum exceeds the value appropriate for PVT by 8-10%, the lowest value attained at $N = 30$ is about 80% of the PVT value. The absence of the inner cells in PSCF tessellations is manifested by a steady increase of the mean values of the size properties.

The variances of the cell size characteristics are very sensitive to small changes in generating point patterns and accessible with a reasonable reliability, too. All of them are monotone increasing, in general, more quickly at low values of N and nearly linearly at above $N \approx 5$ for v and for 2D profile area v'. All variances are higher for PGCF than for BGCF but their difference becomes small at high values of N - Fig 1b. The relative changes with respect to the PVT values are enormous, in particular for globular cluster fields; thus at $N = 30$ is $w \approx 30$ times and $\mathrm{var}\, v \approx 18$ times greater than in PVT. The changes in variances of shape characteristics and factors are smaller; *e.g.* $\mathrm{var}\, g$ increases 8 times and $\mathrm{var}\, n$ only 2 times at maximum. The variances of cell size properties in tessellations generated by PSCF are considerably smaller as a consequence of the absence of inner cells; the reason of their slow growth is the increasing variability of outer cells only.

The development or absence of inner cells can be simply followed by comparing the probability density functions (p.d.f.) of some cell-size property at a small cluster size and gradually increasing N - Fig. 2a. Binomial globular clusters have been chosen here because of their simplicity; note the negligible dependence of the secondary mode on the value of $N \geq 6$. In the tessellations generated by PSCF's (Fig. 2b), small cells are produced by an interaction of closely spaced clusters. They are not true inner cells; their frequency is low, their size is much greater and the relation of their occurrence to N, c is quite different than in the previously described case (*e.g.* for the mean width,

the height of the secondary mode decreases with decreasing cluster size for PSCF with $N = 20$ in contrast to Fig. 5a).

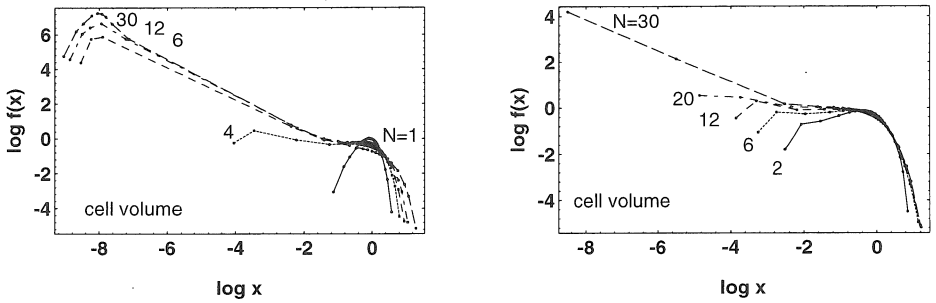

a) b)

Fig. 2 The probability density functions $f_v(x)$ of the cell volume in the tessellations generated by BGCF (a) and PSCF (b); the cluster size $c = 0.005$. The p.d.f's of other cell size properties behave similarly.

The behaviour of the shape properties is much more complex and significant changes in their values take place in particular at small and medium values of N. For example, shape factors continually decrease with growing N but they vary only little above $N \sim 15$. Their values are very similar for both globular cluster fields and they are only slightly higher for the spherical cluster fields. The values $g \sim 0.55$, $f \sim 0.35$ are attained at $N = 30$, $c = 0.005$. The values of the shape factors in the PVT are 0.728 and 0.579, hence much flatter Voronoi cells are generated by cluster fields. Secondary modes either very distinct (factor f - Fig. 4b) or rather spurious (factor g) are again observed.

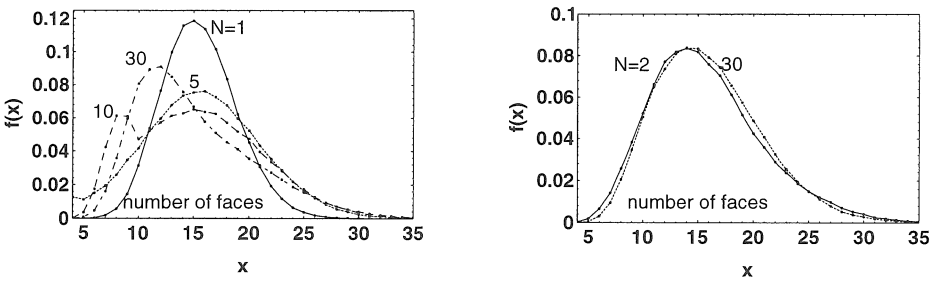

a) b)

Fig. 3 The probability density functions $f_n(x)$ of the number of faces n in the tessellations generated by BGCF (a) and PSCF (b); the cluster size $c = 0.005$.

The behaviour of the number of faces n is very illuminative. The PVT value of N is 15.335 and varies in the interval [15,16] in tessellation generated by cluster fields. It has a small maximum at $N = 2$ and then approaches the value of 15 (globular cluster fields) or, after an increase at small values of N, moves slowly towards the value of 16 (spherical cluster fields). However, its variance has a steep rise at small values of N and a maximum near $N = 5$ for spherical cluster field and near $N = 10$ otherwise.
The shapes of p.d.f's are shown in Fig. 3. First, the primary mode of the distribution shifts to higher values, its height decreases and cells with high number of faces are

created. At the same time a small secondary mode emerges at $x = 4$ and testifies the presence of tetrahedral cells generated by the first inner daughters. For higher N, this mode shifts to higher values of n and its height gradually increases. Finally, a seemingly unimodal positively skewed distribution of n evolves with the mode at $x \approx 10$, which is an important difference between PVT and globular cluster field tessellations. The tail of the distribution is very long and includes the original primary mode; the cells with n exceeding 50 were observed (in PVT, $\max(n) \leq 40$ in samples of comparable size). The maximum of the variance corresponds to the situation in which the distance between the modes is the greatest. Nothing of this kind happens in tessellations with missing inner cells generated by PSCF's - Fig. 3b.

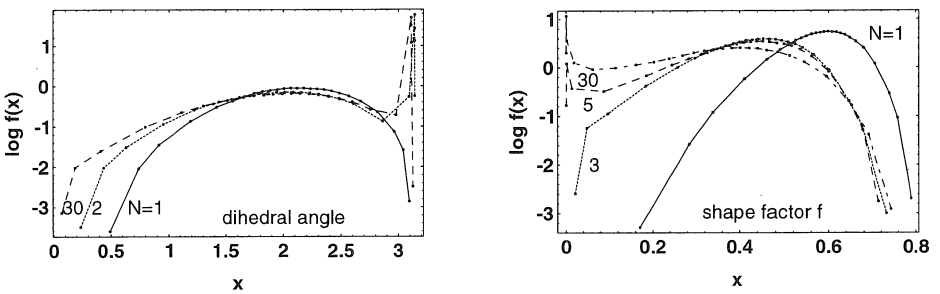

Fig. 4 The probability density functions $f_\theta(x)$ of the random dihedral angle θ (a) and $f_f(x)$ of the shape factor f (b) in the tessellations generated by BGCF; the cluster size $c = 0.005$.

Appealing is also the behaviour of the randomly selected dihedral angle θ (following Lorz and Hahn (1993), one of the edges of any cell is chosen at random and the interior dihedral angle of the adjacent faces is calculated). The mean value $\mathbf{E}\theta$ does not differ substantially from the average (cell) dihedral angle Θ (the average value of all interior dihedral angles in a cell). A sharp secondary mode just bellow $x = \pi$ occurs already for $N = 2$ in all examined cluster tessellation at negligible cluster size - Fig. 4a - and at about $N = 6$ includes as much as 10% of dihedral angles. The peak slightly broadens and shifts to lower values for higher values of N. Its reason are small disturbances of the outer parent cell faces caused by closely spaced daughters of the neighbouring cluster. Its relative importance is weakened by the presence of numerous inner cells at high values of N in the both globular cluster fields. Simultaneously, the frequency of very small angles increases slightly. $\operatorname{var}\theta$ has a shallow maximum at about $N = 6$ for globular cluster fields and continually increases for spherical cluster fields.

Also the distribution of the average dihedral angle Θ change on growing N; namely the originally unimodal distribution with the mode at $\Theta \sim 2\pi/3$ broadens and includes also values of Θ as small as $\pi/3$ at the values of N about 6 (the presence of tetrahedral cells) in BGCF and PGCF tessellations; $\operatorname{var}\Theta$ attains its maximum just at this value of N. The frequency of the small average dihedral angles Θ is distinctly lower in tessellations produced by spherical clusters and $\operatorname{var}\Theta$ continually decreases with growing N.

Shape properties thus sensitively reflect the various differences between PVT and tessellations produced by cluster fields as well as dissimilarities between globular and spherical arrangement of generators. For the latter case, also the shape factor f can be helpful; a sharp mode near $f = 0$ (plate-like inner cells) can be observed only in

tessellations generated by globular clusters - Fig. 4b.

b) The effect of variable cluster size c.

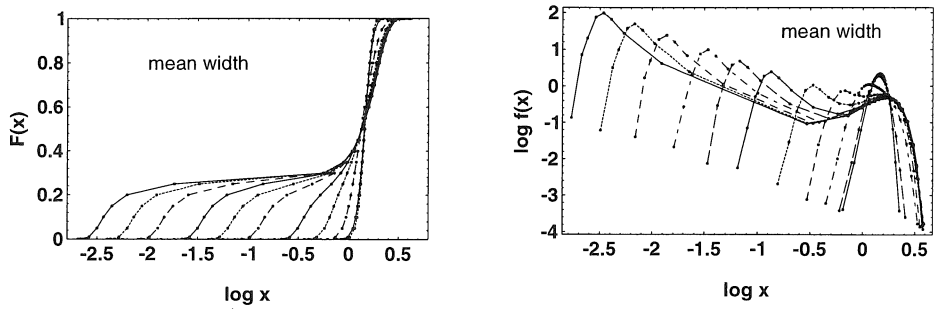

Fig. 5 The distribution function $F_w(x)$ (a) and the p.d.f. $f_w(x)$ (b) of the mean width w in the tessellations generated by PGCF with $N = 20$ and variable cluster size $c_i = 0.005, 0.01, 0.02, 0.05, ..., 5, 10, i = 1, ..., 11$. In the sequence of curves, the cell size parameter increases from the left to the right.

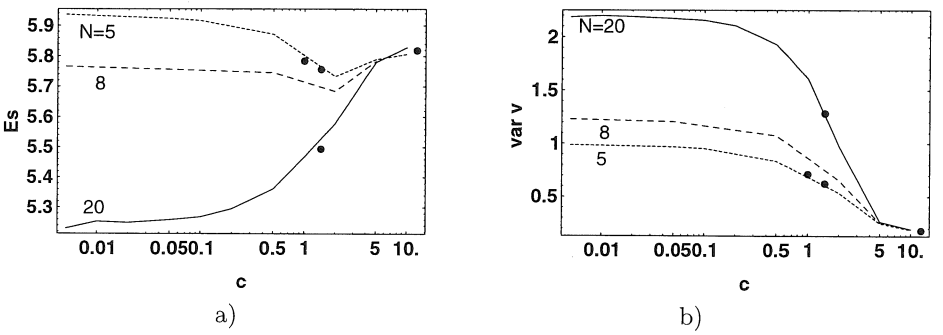

Fig. 6 The mean value $\mathbf{E}s$ (a) of the cell surface and the variance $\mathrm{var}\, v$ (b) of cell volume in the tessellations generated by PGCF with $N = 5, 8, 20$ and variable cluster size c as in Fig. 5. The values obtained by Lorz and Hahn (1993) are denoted by dots, the dots at $c = 11$ show the PVT value.

This effect can be most clearly demonstrated by varying the size c at some chosen fixed value of N - Fig. 5. The ratios of the neighbouring secondary modes of $f_w(x)$ are $x_{i+1} : x_i = c_{i+1} : c_i$, the ratios of heights $f_w(x_{i+1}) : f_w(x_i) = c_i : c_{i+1}$ for $c_{i+1} < 0.5$, i.e. $i < 6$ and c within the cluster size range I. Hence the expectations discussed in the section Preliminary considerations are confirmed and the tessellation generated by very small globular clusters at higher N can be considered as a mixture of small inner cells (their fraction is approximately 25% at $N = 20$, 35% at $N = 30$ for PGCF, slightly lower values hold for BGCF) and large outer cells. Within the range II of cluster sizes, the differences between these two populations gradually vanish and only negligible changes proceed during the further growth in the range III (the narrow unimodal curves in Fig. 5b correspond to $c = 5, 10$). Other size properties change similarly. P.d.f's of shape properties does not change so distinctly, nevertheless all secondary modes gradually vanish in the size range II.

The effects of variable cluster size can also be observed by examining the moments of the cell size characteristics. Three values of N and tessellations induced by PGCF's have been selected; namely $N = 5, 8$ lying in the vicinity of maxima of several characteristics and $N = 20$, for which the mean values of cell size properties are considerably lower than the PVT values. The values $N = 5, 20$ were also chosen for examination of PGCF tessellations by Lorz and Hahn [3]: the lower of them was tested at two values of the overlap parameter $p_1 = 0.5, 0.9$, $N = 20$ only at $p_1 = 0.9$. In terms of the parameter c, these values are 0.99 and 1.46, *i.e.* within the range II. The agreement between the both simulations is very good as shown in Fig. 6.
Again as before, great changes in the properties proceed in the interval of cluster size $0.5 \leq c \leq 5$). Only some characteristics are practically constant in the whole region I , other slowly change even there (in particular for $N = 20$). Whereas the change in variances in the course of the passage from highly clustered tessellations to PVT is monotone as a rule - Fig. 6b, the mean values (and also the values of skewness and kurtosis) frequently pass through maximum or minimum in the range of cluster overlapping as it was already reported for 2D (Saxl and Kohútek, 1997). Their occurrence, height or depth as well as positions vary from one characteristic to another one.

c) Characteristics of induced planar sections.

The well known stereological formulae relate characteristics of the 3D tessellations and of the 2D tessellations induced in planar sections. The 2D intensity $\lambda' = \mathbf{E}w\lambda$, the mean cell area $\mathbf{E}v' = \mathbf{E}v/\mathbf{E}w$ and the mean cell perimeter $\mathbf{E}s' = 0.25\pi\mathbf{E}s/\mathbf{E}w$. (the mutually corresponding quantities are denoted by the same kernel letter and the prime in 2D). Consequently, the 2D characteristics are again homogeneous function of degree k' of the 3D intensity λ. The degree is $k' = -\frac{2}{3}, -\frac{1}{3}$ for v', s', resp. and $k' = \frac{2}{3}$ for λ'. The planar shape characteristics are number of edges n', randomly selected edge angle θ', mean edge angle Θ' and shape factor $f' = 4\pi v'/s'^2$.

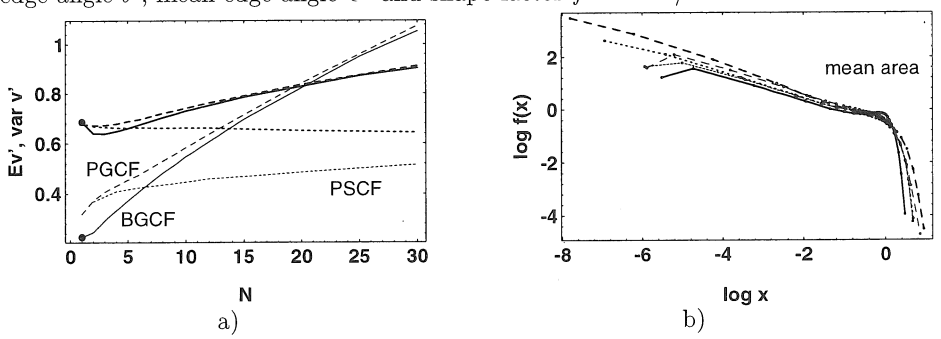

Fig. 7 (a) The mean value $\mathbf{E}v'$ (thick lines) of the cell area and the variance var v' (thin lines) of cell area in 2D sections of 3D tessellations: $c = 0.005$. (b) The p.d.f's of the cell area v' for the PVT (full line) and $N = 2$ (dotted), 20 (dashed) in 2D sections of 3D tessellations generated by PGCF (thick lines) and PSCF (shorter thin lines); $c = 0.005$.

As $\mathbf{E}v = 1$, $\mathbf{E}v'$ is just a reciprocal value of $\mathbf{E}w$ as a consequence of the above mentioned stereological formula - Fig. 7a. The mean perimeter $\mathbf{s}'$ behaves similarly and the variances of the both sectional size characteristics increase with growing N analogically as the variances of 3D cell characteristics - Fig. 7a.

Whereas the inner and outer cells are clearly distinguished in bimodal p.d.f's of 3D cell characteristics, the sectional characteristics are much less explicit. The reason lies in sampling the 3D cell population by the sectioning plane. Denoting by q the ratio of inner (i) and outer (o) cell intensities in 3D, then in the section plane $q' = \lambda_i'/\lambda_o' = q\mathbf{E}w_i/\mathbf{E}w_o$. The ratio of the mean widths of inner and outer particles is approximately proportional to $(\lambda/\lambda_d)^{1/3} \sim c$. Hence if q is about 0.25 for $N = 20$ and $c = 0.005$, then $q' \sim 0.001$, and sections of inner cells are very rare. Moreover, the p.d.f. of cell area is bimodal (with a secondary mode near $x \approx 0$) even in PVT as shown by Hahn and Lorz (1993). Therefore the main manifestation of the presence of inner cells is the extension of the cell area p.d.f. to smaller values and the disappearance of the primary mode - Fig. 7b. A little more revealing is the p.d.f. of planar cell perimeter s' - Fig. 8a. A very shallow secondary mode is apparent here owing to the unimodality of the p.d.f. in the tessellation induced by PVT.

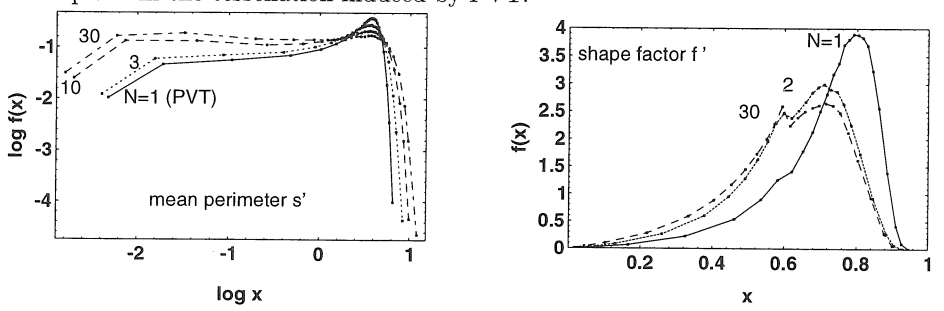

Fig. 8 The p.d.f's of the cell perimeter s' (a) and of the shape factor f' (b) in 2D sections of 3D tessellations generated by BGCF cluster field: $c = 0.005$.

All sectional shape characteristics change again mainly in the region of small values of N. n' is unimodal for all N with the obligatory mean value $\mathbf{E}n' = 6$. The only discernible differences between generating cluster fields are a higher probability of cells with small and high n' and a less sharp mode at $n \sim 6$ for globular fields, an increasing sharpness of the mode with N for spherical fields (at $N = 30$, a slightly narrower PVT shape is approached) and, accordingly, a lower variance in the latter case. $f_\theta'(x)$ is bimodal with a secondary maximum near $x = \pi$, the probability of small angles is higher and the primary mode is shifted to smaller values in sections of PGCF and BGCF tessellations. $\mathbf{E}\theta'$ is not much affected by the value of N above 3, its variance is nearly twice as high as in PVT and nearly constant for $N > 10$ (it is slightly smaller for PSCF as the broadening of the secondary maximum is not accompanied by the increasing probability of small angles). The p.d.f's are very stable within the whole range I of cluster sizes and the secondary mode is discernible even at $c = 2$. The shape factor f' is bimodal even in PVT with modes $x = 0.8$ (primary mode), 0.6 (Lorz and Hahn, 1993). However, the primary mode shifts to 0.7 and the secondary mode is much more pronounced in tessellations generated by all considered cluster fields - Fig. 8b. Hence a reason of such a more distinct bimodality must lie in the shape of outer cells and, consequently, the mean values $\mathbf{E}f'$ are very similar for globular as well as spherical cluster fields: the mean values roughly about 15% lower than in PVT are attained already at $N = 4$ and very slowly decrease with growing N. The variances var f' are nearly constant and higher only by 10% than in PVT.

CONCLUSIONS

Three examined variables of cluster fields, namely arrangement of daughters, cluster size and number of daughters, substantially influence the generated 3D Voronoi tessellations as well as their planar sections.

The cluster size is the most important parameter and if it exceeds considerably the mean nearest neighbour distance between the parents (size range III) then the difference between examined tessellation and PVT cannot be reliably recognized however large the number of daughters is or however disparate their arrangements are. On the other hand, a further decrease of cluster size below some small fraction of the parent nearest neighbour distance (size range I) influences many characteristics only weakly and the mean number of daughters is the controlling parameter.

A prominent feature of the majority of examined distributions of cell characteristics is the bimodality. It can serve as a basis of qualitative (presence of clusters, daughter arrangement) as well as quantitative (cluster size, mean number of daughters) estimates of the point field properties. Cell size properties are bimodal due to the presence of inner cells developed in the cluster core when the number of daughters is high. An extreme proximity of daughters generating outer cells invokes an important secondary mode of the random internal angles θ, θ', plate-like inner cells initiate a secondary mode of the shape factor f. The complex behaviour of the face number distribution is also closely connected with the presence of inner cells. Unexplained remains the bimodality of the sectional shape factor f' recognizable even in PVT.

A preliminary knowledge stemming from the qualitative analysis of property distributions is important for more reliable estimates derived from the moments of various properties as the effect of the cluster size and of the daughter number is not monotone, in particular for odd moments and quantities based on it. Fortunately enough, variances of cell size properties behave regularly: a monotone, significant and clearly discernible even in planar sections increase of variances with growing N and their decrease with growing cluster size can serve as a reliable base of estimation.

REFERENCES

Hahn U, Lorz U: Stereological analysis of the spatial Poisson-Voronoi tessellation. J Microsc 1994; 175: 176-185.

Lorz U: Cell-area distributions of planar sections of spatial Voronoi mosaics. Materials Characterization 1990; 25: 297-311.

Lorz U, Hahn U: Geometric characteristics of random spatial Voronoi tessellations and planar sections. Preprint 93-05. Freiberg: Bergakademie Freiberg, 1993.

Okabe A, Boots B, Sugihara K: Spatial tessellations. Chichester: J.Wiley & Sons, 1992.

Rataj J, Saxl I: Boolean Cluster Models. Mathematica Bohemica 1997: 122: 21-36.

Saxl I, Kohútek I: Voronoi tessellations generated by Boolean cluster fields. In: Wojnar L, Rożniatowski K, Kurzydłowski K(eds.): Proc Int Conf on The Quantitative Description of Materials Microstructure. Warsaw , April 1997, 481-488.

Saxl I, Ponížil P: Estimation of propertis of polycrystalline grain structure. In: L. Parilák (ed.): Fractography 97. Proc Int Conf, Vysoké Tatry. ÚMV SAV Košice 1997, 132-144.

Stoyan D, Kendall WS, Mecke J: Stochastic Geometry and its Applications. New York: J Wiley & Sons, 1995.

Presented at the 7th European Congress for Stereology, Amsterdam, April 20th to 23rd, 1998.